

## Two mechanisms of exciton dissociation in rubrene single crystals

Hikmat Najafov, Byunggook Lyu, Ivan Biaggio, and Vitaly Podzorov

Citation: *Appl. Phys. Lett.* **96**, 183302 (2010); doi: 10.1063/1.3421539

View online: <http://dx.doi.org/10.1063/1.3421539>

View Table of Contents: <http://apl.aip.org/resource/1/APPLAB/v96/i18>

Published by the [American Institute of Physics](#).

---

### Related Articles

Trapping photon-dressed Dirac electrons in a quantum dot studied by coherent two dimensional photon echo spectroscopy

*J. Chem. Phys.* **136**, 194106 (2012)

Surface sensing behavior and band edge properties of AgAIS<sub>2</sub>: Experimental observations in optical, chemical, and thermorefectance spectroscopy

*AIP Advances* **2**, 022123 (2012)

Excitation power and temperature dependence of excitons in CuInSe<sub>2</sub>

*J. Appl. Phys.* **111**, 093507 (2012)

Magnetoexcitons and optical absorption of bilayer-structured topological insulators

*Appl. Phys. Lett.* **100**, 161602 (2012)

Temperature and composition dependence of photoluminescence dynamics in CdS<sub>x</sub>Se<sub>1-x</sub> (0 ≤ x ≤ 1) nanobelts

*J. Appl. Phys.* **111**, 073112 (2012)

---

### Additional information on *Appl. Phys. Lett.*

Journal Homepage: <http://apl.aip.org/>

Journal Information: [http://apl.aip.org/about/about\\_the\\_journal](http://apl.aip.org/about/about_the_journal)

Top downloads: [http://apl.aip.org/features/most\\_downloaded](http://apl.aip.org/features/most_downloaded)

Information for Authors: <http://apl.aip.org/authors>

## ADVERTISEMENT



**Goodfellow**  
metals • ceramics • polymers • composites  
70,000 products  
450 different materials  
**small quantities fast**

[www.goodfellowusa.com](http://www.goodfellowusa.com)

## Two mechanisms of exciton dissociation in rubrene single crystals

Hikmat Najafov,<sup>1</sup> Byunggook Lyu,<sup>1</sup> Ivan Biaggio,<sup>1,a)</sup> and Vitaly Podzorov<sup>2</sup>

<sup>1</sup>Department of Physics and Center for Optical Technologies, Lehigh University, Bethlehem, Pennsylvania 18015, USA

<sup>2</sup>Department of Physics and Astronomy, Rutgers University, Piscataway, New Jersey 08854, USA

(Received 18 December 2009; accepted 12 April 2010; published online 5 May 2010)

Excitons in rubrene single crystals dissociate into free charge carriers via two mechanisms whose relative importance depends on the illumination wavelength through the optical penetration depth into the crystal. The first mechanism is defect-induced dissociation in less than 10 ns after photoexcitation. For low photoexcitation densities, about 10% of the excitons that survive radiative recombination dissociate through this channel. The second mechanism, affecting the remaining 90% of the excitons, involves a previously reported state localized close to the surface of the crystal that leads to a delayed release of photocarriers a fraction of a millisecond after photoexcitation. © 2010 American Institute of Physics. [doi:10.1063/1.3421539]

One of the remarkable phenomena observed in rubrene single crystals is a delayed release of charge carriers that occurs several tens of microseconds after the initial photoexcitation of a molecular exciton and long after the decay of the excitonic luminescence.<sup>1,2</sup> The dependence of the photoconductivity dynamics on both the wavelength and the intensity of pulsed optical excitation is consistent with an efficient transfer of the initial excitation to a defect-related state that has a higher density close to the surface of the crystal and that later releases holes (the carriers with the largest mobility in rubrene)<sup>3</sup> at a constant rate.<sup>1,2</sup> The released holes are then free to drift in the applied field until they recombine with the electrons they left behind. This delayed photocurrent response is the dominant effect for low-intensity pulsed illumination of rubrene.<sup>2</sup>

In this work we investigate the origin of a fast photocurrent component that builds up in less than 10 ns and is about ten times weaker than the delayed component but becomes more important at higher excitation densities when the delayed component saturates.

The experimental setup consists of a rubrene crystal with two graphite contacts deposited on the (a,b) facet of the crystal, 2 to 5 mm apart. The laser pulses illuminate a spot with a diameter of 0.3 mm in the middle between the contacts. An electric field of the order of 2 kV/cm is applied to the contacts, which are connected in series to a resistor  $R_s$  over which we measure the time-dependent voltage drop with a 4 GHz LeCroy oscilloscope. Given the capacitance  $C$  in the circuit, mostly due to the cables we use, the response time of the current measurement varies from  $R_s C \sim 5$  ns for  $R_s = 50 \Omega$  to  $R_s C \sim 5 \mu\text{s}$  for  $R_s = 5 \text{ k}\Omega$ , used when measuring the slower dynamics of weaker photocurrents.

We illuminated the sample with 20 ps long laser pulses in a wavelength range between 580 and 600 nm, close to the onset of molecular absorption in the rubrene crystal.<sup>1</sup> We chose this illumination wavelength because it corresponds to an absorption length in the sample of  $\sim 100 \mu\text{m}$ , guaranteeing that we create molecular excitons in a relatively thick surface layer. Rubrene is a molecular crystal with molecules bound by Van der Waals forces, and light absorption prima-

rily results in a localized transition where a molecule is promoted to an excited state, thus directly forming molecular excitons.<sup>1,4-6</sup>

The inset in Fig. 1 shows examples of the observed photocurrent dynamics. At higher pulse energies a fast photocurrent component can be clearly seen. Its buildup time is faster than 10 ns, given by the time-resolution of our equipment. We analyzed the photocurrent transients by extracting (1) the amplitude of the fast current component  $p(0)$ ; (2) the maximum amplitude  $p_{\text{max}}$ ; (3) the exponential buildup time of the slow component rising from  $p(0)$ . The results are plotted together in Fig. 1 for two different illumination wavelengths as a function of the absorbed photon density at the surface of the crystal. The latter is derived from pulse energy, wave-

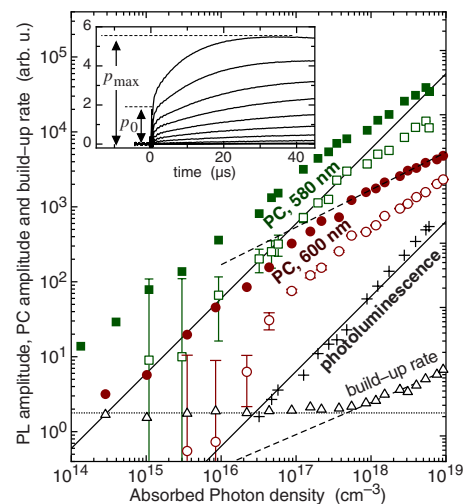


FIG. 1. (Color online) Inset: typical photocurrent transients observed after illumination with 20 ps pulses at 600 nm wavelength, showing a delayed photocurrent buildup and a fast buildup that occurs in less than 10 ns, and an increase in current for growing pulse energies in the high-exposure region above an absorbed photon density of  $10^{17} \text{ cm}^{-3}$ . Main figure: dependence of the maximum photocurrent ( $p_{\text{max}}$ , filled symbols) and of its fast component ( $p_0$ , open symbols) on the absorbed photon density at the surface of the crystal. Green squares and red circles are for illumination wavelengths of 580 nm and 600 nm, respectively. The crosses represent the photoluminescence intensity, and the triangles are the buildup rate of the photocurrent. The solid lines represent a linear dependence and the dashed lines represent a square-root dependence.

<sup>a)</sup>Electronic mail: biaggio@lehigh.edu.

length dependent absorption, and the illuminated area, which was  $\sim 7 \times 10^{-4} \text{ cm}^2$ .

The pulse energy dependence of the peak current and the buildup rate of the delayed component is the expected one, as described in Ref. 2, with a transition from a low to a high exposure regime where they both grow as the square root of the pulse energy, an effect caused by the quadratic recombination of released charge carriers.<sup>2</sup>

At low exposures (below an absorbed photon density of  $\sim 10^{17} \text{ cm}^{-3}$ , see Fig. 1), both fast photocurrent component and total amplitude grow linearly with illumination pulse energy, with the fast component contributing about 10% to the total current amplitude reached later, on the microsecond time-scale. At the lowest exposures (and for both 600 and 580 nm illumination) the fast component disappears into the noise, with no sign of a threshold for its appearance or of a superlinear dependence from the excitation energy. As the pulse energy increases, the growth of the fast component becomes sublinear but this saturation occurs at higher exposures than for the delayed component, as proven by the very clear continuing growth of the ratio  $p(0)/p_{\text{max}}$  over the pulse energy range we studied. At even higher pulse energies quadratic recombination becomes increasingly important, and the combination of the shortening of the buildup time of the delayed current and its saturation<sup>2</sup> lead to a photocurrent trace where the two photocurrent components cannot be easily distinguished anymore.

We note that the photoluminescence excited at 580 nm keeps growing linearly for the entire range of pulse energies we used, without any signs of saturation in correspondence with the appearance of the instantaneous component of the photocurrent or anywhere else.

The linearity of the fast photocurrent component at lower exposures, with no observable threshold effect, and the absence of any saturation in the photoluminescence intensity lead us to rule out the possibility that the fast release of the carriers during the first 10 ns is associated with any kind of high density effect such as, for example, exciton autoionization by exciton-exciton interaction.<sup>7-9</sup>

We assign the two components of the photocurrent to two independent exciton dissociation mechanisms, but before discussing their origin we need to mention and eliminate another possibility. Because of previous observations under different experimental conditions of a free carrier signal that appears and decays on the picosecond scale,<sup>10</sup> it may be tempting to interpret the fast photocurrent that we observe as caused by a density  $N_0$  of short-lived photoinduced charge carriers that are quickly trapped in a shallow trap level. On longer time scales, they would then be thermally reexcited to continue contributing to the photocurrent with an effective (trap-limited) mobility  $\mu_t$ . While such an effect cannot explain the delayed buildup of the photocurrent, a photoinduced carrier population decaying as  $N_0 \exp(-t/\tau)$  with  $\tau \ll R_s C$  would lead to a step-wise increase in the voltage drop over the resistor  $R_s$  (with an exponential buildup time  $\tau$ ) and a size of the step  $V_s$  proportional to the time integral of the fast photocurrent transient divided by the capacitance in the circuit,<sup>11</sup>

$$V_s = \frac{\tau}{C} \times \frac{eN_0\mu_0 E}{d}, \quad (1)$$

where  $e$  is the unit charge,  $\mu_0$  is the free carrier mobility,  $E$  is the applied electric field, and  $d$  is the distance between the contacts. On the other hand, the voltage drop on the resistor due to a total number of carriers  $N_t$  that exists between the contacts at times much larger than  $R_s C$  is just the product of  $R_s$  and the current,

$$V_D = R_s \times \frac{eN_t\mu_t E}{d}, \quad (2)$$

where we allowed for a different (possibly trap limited) mobility  $\mu_t$ . Hence, under these measurement conditions the ratio between the voltage drop seen at times  $t \ll R_s C$  and that seen at times  $t \gg R_s C$  is

$$\frac{V_s}{V_D} = \frac{\tau}{R_s C} \frac{N_0 \mu_0}{N_t \mu_t}. \quad (3)$$

This means that under such a scenario the relative size of fast photocurrent amplitude and delayed photocurrent would depend on the measurement resistor, which is not the case for our data: All photocurrent transients we observed do not change their shape when  $R_s$  is varied. It follows that the initial fast photocurrent component must be due to exciton dissociation into long-lived carriers that are indistinguishable from those which are released later to create the delayed photocurrent. This supports the conclusion that the two components of the photocurrent are related to two different exciton dissociation mechanisms. While the delayed photocurrent component is due to exciton interaction with the previously described defect state close to the surface of the crystal,<sup>2</sup> the fast photocurrent is likely due to defect-induced dissociation of the singlet exciton during its lifetime of less than 10 ns. A direct excitation of a small density of free charge carriers by the laser pulse, which would also be consistent with our data, is not compatible with the view that photoexcitation in molecular crystals results in molecular excitons.<sup>4-6</sup>

The amplitude of both components of the current increases significantly in correspondence with the onset of the excitonic absorption for wavelengths decreasing below 600 nm, which also proves that the creation of excitons is a prerequisite for both components of the photocurrent. On the other hand, excitonic absorption close to the band gap competes with other absorption mechanisms, such as impurity absorption, that vary from sample to sample. Indeed, we observed significant sample-dependent variations in the details of the wavelength dependence of the two photocurrent components as the wavelength is varied toward the infrared. Sample-to-sample variations are also observed in the amplitude of the two photocurrent components, with somewhat more variability in the delayed component. In any case, for each individual sample the wavelength dependence of fast and delayed component are not directly correlated. All this again supports the conclusion that while both photocurrent components originate from photoexcited excitons, the mechanisms of exciton dissociation responsible for the fast and delayed photocurrent are independent from each other.

An additional proof of the different origins of fast and delayed photocurrent was obtained by application of the gauge effect to the surface of photoconducting rubrene

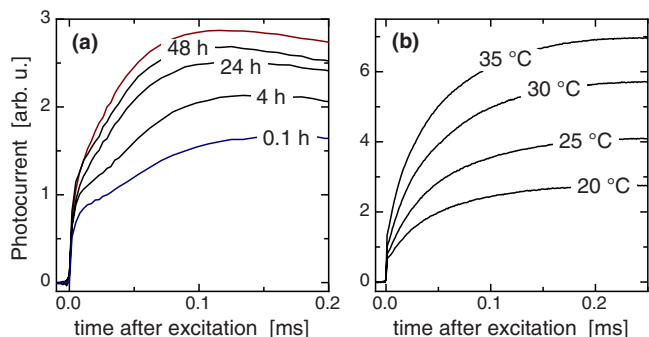


FIG. 2. (Color online) (a) Changes in the photocurrent dynamics induced by 600 nm pulsed illumination before and after a short exposure of the crystal surface to free radicals created by a high vacuum gauge (see Ref. 12). The curve with the largest amplitude was obtained before exposure to the gauge effect. The other curves are labeled with the time in hours after the sample was removed from the vacuum environment. (b) Changes in photocurrent dynamics with temperature, measured in another sample. Each curve is labeled with the temperature in degree celsius.

samples.<sup>12</sup> This effect allows to selectively hinder charge transport close to the surface of rubrene crystals. It is caused by free radicals, created by high vacuum gauges, which rapidly attack the surface of a crystal held in the vacuum enclosure.<sup>12</sup> We observed that within a few seconds after activating the ion-gauge the delayed photocurrent component decreased by more than a factor of 2, while the fast component (the “step” in the photocurrent buildup) decreased by less than 25% [Fig. 2(a)]. The photocurrent then slowly recovers on a time-scale of a few hours after exposure of the sample to air, in accordance with earlier measurements of the dark conductivity.<sup>12</sup> The higher sensitivity of the delayed photocurrent to the gauge effect proves that this conduction takes place closer to the surface of the crystal, consistent with our earlier assignment of this delayed photocurrent to exciton interaction with a defect state localized within a few micrometers from the surface.<sup>2</sup> At the same time, the significantly smaller sensitivity to the gauge effect of the fast photocurrent component proves that it originates deeper inside the bulk of the crystal. It is likely to be caused by defect-induced exciton dissociation with a homogenous distribution of defect sites in the bulk. The surface-sensitivity of the gauge effect was also confirmed by the fact that gauge-induced reduction in the photocurrent was 5 to 10 times larger when illuminating close to the peak absorption of rubrene near 495 nm, where the penetration length of the light is  $\sim 1 \mu\text{m}$ . Similar independent evolutions of the strengths

of the fast and delayed photocurrent components can be observed when increasing the sample temperature. Figure 2(b) shows that an increase in temperature of only 15 °C causes the delayed component to grow by a factor of 3 (consistent with the previous results reported in Ref. 2) while the change in the amplitude of the fast component is less than a factor of 2 over the same temperature interval.

In conclusion, rubrene single crystals are characterized by two distinct exciton dissociation mechanisms: one mechanism leads to dissociation of the exciton during its lifetime, and is probably caused by interaction with bulk defects, while the other mechanism is related to surface oxidation, with an emission of free carriers that occurs several tens of microseconds after the creation of the exciton.<sup>2</sup> While the exact nature of the defects and surface-states responsible for exciton dissociation is not completely clear yet, further studies on rubrene and its excitons should be very interesting for the insights they can give on important excitonic processes in molecular crystals.

This research at Lehigh has been supported by the donors of the American Chemical Society Petroleum Research Fund (Grant No. 45741-AC10). The work at Rutgers has been supported by NSF under Grant Nos. DMR-0843985 and ECS-0822036.

<sup>1</sup>H. Najafov, I. Biaggio, V. Podzorov, M. F. Calhoun, and M. E. Gershenson, *Phys. Rev. Lett.* **96**, 056604 (2006).

<sup>2</sup>H. Najafov, B. Lyu, I. Biaggio, and V. Podzorov, *Phys. Rev. B* **77**, 125202 (2008).

<sup>3</sup>V. Podzorov, V. M. Pugalov, and M. E. Gershenson, *Appl. Phys. Lett.* **85**, 6039 (2004).

<sup>4</sup>M. Pope and C. E. Swenberg, *Annu. Rev. Phys. Chem.* **35**, 613 (1984).

<sup>5</sup>E. A. Silinsh and V. Capek, *Organic Molecular Crystals: Interaction, Localization, and Transport Phenomena* (American Institute of Physics, New York, 1994).

<sup>6</sup>M. Pope and C. E. Swenberg, *Electronic Processes in Organic Crystals and Polymers* (Oxford University Press, New York, 1999).

<sup>7</sup>M. Silver, D. Olness, M. Swicord, and R. C. Jarnagin, *Phys. Rev. Lett.* **10**, 12 (1963).

<sup>8</sup>C. L. Braun, *Phys. Rev. Lett.* **21**, 215 (1968).

<sup>9</sup>T. E. Orlovski and H. Scher, *Phys. Rev. B* **27**, 7691 (1983).

<sup>10</sup>O. Ostroverkhova, D. G. Cooke, F. A. Hegmann, J. E. Anthony, V. Podzorov, E. Gershenson, O. D. Jurchescu, and T. T. M. Palstra, *Appl. Phys. Lett.* **88**, 162101 (2006).

<sup>11</sup>A. Taponnier, I. Biaggio, M. Koehler, and P. Günter, *Appl. Phys. Lett.* **83**, 5473 (2003).

<sup>12</sup>V. Podzorov, E. Menard, S. Pereversev, B. Yakshinsky, T. Madey, J. A. Rogers, and M. E. Gershenson, *Appl. Phys. Lett.* **87**, 093505 (2005).